

Frequency-Aligned Knowledge Distillation for Lightweight Spatiotemporal Forecasting

Yuqi Li^{1*}, Chuanguang Yang^{1*}, Hansheng Zeng², Zeyu Dong¹,
Zhulin An¹, Yongjun Xu¹, Yingli Tian³, Hao Wu^{4†}

¹Institute of Computing Technology, Chinese Academy of Sciences

²The University of Hong Kong

³The City University of New York

⁴Tsinghua University

Abstract

Spatiotemporal forecasting tasks, such as traffic flow, combustion dynamics, and weather forecasting, often require complex models that suffer from low training efficiency and high memory consumption. This paper proposes a lightweight framework, Spectral Decoupled Knowledge Distillation (termed SDKD), which transfers the multi-scale spatiotemporal representations from a complex teacher model to a more efficient lightweight student network. The teacher model follows an encoder-latent evolution-decoder architecture, where its latent evolution module decouples high-frequency details and low-frequency trends using convolution and Transformer (global low-frequency modeler). However, the multi-layer convolution and deconvolution structures result in slow training and high memory usage. To address these issues, we propose a frequency-aligned knowledge distillation strategy, which extracts multi-scale spectral features from the teacher’s latent space, including both high and low frequency components, to guide the lightweight student model in capturing both local fine-grained variations and global evolution patterns. Experimental results show that SDKD significantly improves performance, achieving reductions of up to 81.3% in MSE and in MAE 52.3% on the Navier-Stokes equation dataset. The framework effectively captures both high-frequency variations and long-term trends while reducing computational complexity. Our codes are available at <https://github.com/itsnotacie/SDKD>

1. Introduction

Spatiotemporal forecasting, such as traffic flow [15, 23, 36, 46] prediction and weather evolution modeling [2, 47, 48], is a core task for real-time decision-making in smart cities and climate science [22]. These tasks require modeling the complex coupling between high-frequency local patterns (e.g., sudden traffic congestion) [6] and low-frequency global evolution (e.g., slow atmospheric pressure changes) [32]. Recently, hybrid architectures combining convolutional neural networks (CNNs) and Transformers have achieved state-of-the-art forecasting accuracy by capturing both local features and long-range dependencies [36, 38]. However, as shown in Table 1, their deep stacked structures and complex operators (e.g., multi-head attention with quadratic complexity $O(N^2d)$) lead to prohibitive computational costs and memory consumption (e.g., $3d^2$ parameters per attention layer), making them difficult to deploy in resource-constrained environments such as edge devices. Although model compression techniques like knowledge distillation (KD) offer potential solutions, existing KD frameworks—mainly designed for classification tasks [39, 40, 42]—perform poorly when directly applied to spatiotemporal forecasting. The fundamental reason lies in the multi-band spectral characteristics of continuous spatiotemporal signals, where simple feature imitation fails to maintain the critical balance between high-frequency details and low-frequency trends.

Traditional approaches attempt to decouple spatial and temporal modeling through inductive bias of CNNs/RNNs (e.g., ConvLSTM [31] for localized spatial correlations and PredRNN [35] for sequential dynamics). However, these methods inherently struggle to model cross-scale interactions—the intricate coupling between high-frequency transients (e.g., abrupt traffic surges) and low-frequency trends (e.g., diurnal periodicity). While hybrid CNN-Transformer architectures [36] mitigate this by jointly capturing local-

*Equal Contribution.

†Corresponding Author.

global dependencies, their computational complexity scales quadratically with sequence length (see Table 1), rendering them impractical for long-horizon forecasting. Prior knowledge distillation (KD) methods for regression tasks, such as feature mimicry [28] or output distribution alignment [45], further exacerbate this issue by ignoring the spectral bias inherent in spatiotemporal signals. For instance, distilling high-level semantic features disproportionately suppresses low-frequency components critical for long-term consistency [21], while naive parameter reduction in lightweight architectures (e.g., depthwise separable convolutions [30]) sacrifices generalizability across heterogeneous domains (e.g., fluid dynamics vs. urban mobility). **This dual challenge of efficiency-accuracy trade-off and spectral imbalance underscores the need for a principled distillation framework that explicitly preserves multi-scale spatiotemporal patterns.**

► **Key Gap.** Existing approaches suffer from a fundamental spectral entanglement dilemma: *the absence of explicit mechanisms to decouple and transfer frequency-specific knowledge across spatiotemporal scales.* This leads to a paradoxical trade-off in lightweight models—either over-smoothing high-frequency variations (e.g., traffic surge spikes) through excessive low-pass filtering [27], or failing to capture slow-evolving trends (e.g., seasonal climate shifts) due to high-frequency dominance in parameter updates [4]. While recent attempts like frequency-aware KD [49] apply static spectral masks for classification tasks, they ignore the non-stationary spectral properties of spatiotemporal dynamics, where optimal frequency bands evolve both spatially (e.g., urban vs. rural regions) and temporally (e.g., peak vs. off-peak hours).

We propose **SDKD** (Spectral Decoupled Knowledge Distillation), a principled framework that bridges the efficiency-accuracy gap by compressing complex spatiotemporal teachers into deployable lightweight students through frequency-aware representation alignment. Our core insight stems from the spectral duality of spatiotemporal signals: they inherently comprise *high-frequency components* (localized rapid variations, e.g., traffic congestion spikes) governed by spatial locality, and *low-frequency components* (global slow dynamics, e.g., diurnal traffic periodicity) dominated by temporal continuity [4, 17]. SDKD exploits this duality through two synergistic innovations:

► **Teacher Design with Spectral Disentanglement.** We architect the teacher model as a frequency-aware autoencoder, where CNNs act as *high-pass filters* to capture fine-grained spatial patterns through localized gradient operations [1, 34], while Transformers serve as *low-pass filters* to model global temporal trends via attention-based trend decomposition [24, 26]. This explicit frequency decoupling in the latent space creates disentangled spectral priors—a critical foundation for effective distillation.

► **Architecture-Independent Spectral Transfer.** Traditional

knowledge distillation methods rely on specific architectures to transfer knowledge. However, in spatio-temporal prediction tasks, different student models (e.g., U-Net, ResNet) have different structural characteristics and handle spectral information in various ways. Therefore, we propose an architecture-independent spectral transfer mechanism, which focuses on directly aligning spectral features for knowledge transfer, rather than on the student model’s structure.

► **Contributions Summary.** This paper proposes a systematic solution to balance efficiency and accuracy while addressing spectral imbalance in spatiotemporal forecasting. The main contributions are as follows:

- **Spectral-Decoupled Teacher Architecture:** This paper introduces a frequency-unraveling teacher model with a convolution-Transformer serial design. It explicitly separates high-frequency details (local gradient response) from low-frequency trends (global attention modeling) to construct interpretable spectral priors. Theoretical analysis [24] shows that this design aligns the spectral energy distribution in the latent space with physical laws.
- **Frequency-Aligned Distillation Mechanism:** This paper designs a cross-scale spectral feature alignment loss. It uses multi-band components from the teacher’s latent space as dynamic supervision signals to guide the student model in capturing transient fluctuations and evolutionary trends. This mechanism applies spectrum-sensitive adaptive weighting to mitigate the student model’s inherent high-frequency overfitting and low-frequency underfitting.
- **Excellent Performance:** Experiments show that ST-AlterNet performs better than SimVP, especially on the Weatherbench dataset, with higher MAE, PSNR, and SSIM scores. Using the AEKD strategy (especially AB Loss or MSE Loss) significantly improves student models such as U-Net, ResNet, and MLP-Mixer in MAE and SSIM. For example, U-Net with AEKD (AB Loss) achieves MAE=0.8541, PSNR=31.4527, and SSIM=0.8812 on Weatherbench, showing the effectiveness of AEKD in improving student performance.

This framework provides a general paradigm for high-accuracy spatiotemporal forecasting in resource-limited scenarios.

Table 1. Model Complexity and Parameter Count (N : sequence length, d : channels, K : kernel size, $|E|$: edges)

Model	FLOPs	Parameters	Description
CNN	$K^2 d^2 N$	$K^2 d^2 + d$	Local filtering
RNN (LSTM)	$8d^2 N$	$4d^2 + 4d$	Temporal modeling
Self-Attention	$N^2 d + 3Nd^2$	$3d^2$	Global context
GNN	$ E d + Nd^2$	$d^2 + d$	Graph propagation
FNO	$Nd^2 + Nd \log N$	Nd^2	Spectral conv.

2. Related Work

Spatiotemporal Forecasting Models. The core challenge in spatiotemporal forecasting is modeling the complex coupling between local spatial patterns and global temporal evolution in dynamic systems. Early works optimized efficiency by separating spatial and temporal modeling. ConvLSTM [31] introduced convolution into LSTM to capture spatial correlations, while PredRNN [35] stacked memory units to enhance temporal modeling. However, these methods struggle with cross-scale interactions, such as synchronizing high-frequency transient fluctuations and low-frequency trends. Recently, hybrid architectures (e.g., CNN-Transformer) improved forecasting accuracy by integrating local convolution and global attention mechanisms [36], but their quadratic computational complexity and high memory cost limit practical deployment. To improve efficiency, HPF [25] introduced a lightweight temporal modeling module but sacrificed the ability to capture high-frequency details. Unlike these approaches, this paper reconstructs the modeling paradigm from a frequency-domain decoupling perspective, using knowledge distillation to balance accuracy and efficiency.

Knowledge Distillation Techniques. Knowledge distillation (KD) [18, 19, 41, 43] compresses models by transferring knowledge from a complex teacher model to a lightweight student model. Traditional KD methods focus on classification tasks, transferring knowledge through softened label distributions [11] or intermediate feature matching [14]. For regression tasks, FitNet-R [28] aligns multi-scale features, but directly applying it to spatiotemporal forecasting often causes high-frequency information loss due to spectral bias. Recent studies incorporate frequency-domain analysis to improve distillation. FOLK [16] separates high and low frequency knowledge using frequency masks in image classification but ignores the continuity of spatiotemporal signals. STGNN-Distill [12] enhances long-range dependency modeling through spatiotemporal attention distillation but still relies on complex attention mechanisms. This paper introduces the first decoupled distillation framework tailored for spatiotemporal signals, enabling cross-scale knowledge transfer through a frequency-domain alignment strategy.

Frequency-Domain Representation Learning. Frequency domain analysis provides a theoretical tool for understanding the spectral preferences of deep networks. Jacot et al. [13] showed that CNNs exhibit an inductive bias toward low-frequency components through neural tangent kernel theory, while Transformers, due to their self-attention mechanism, capture high-frequency details more effectively [3]. Following this, FNO [17] models partial differential equations using Fourier operators but struggles with non-stationary spatiotemporal signals. SFNet [5] decouples multi-scale features using wavelet transforms, but its manually designed filters lack adaptability. Unlike explicit frequency-domain modeling, this paper leverages a teacher model with implicit

spectral decoupling to provide prior knowledge, allowing the student model to inherit multi-scale representations without complex frequency-domain operations. This approach introduces a new paradigm for lightweight spatiotemporal forecasting.

Key Differences. Existing works either rely on complex hybrid architectures that sacrifice efficiency (e.g., CNN-Transformer), simplify models at the cost of fine-grained dynamics (e.g., FOLK), or use generic distillation strategies unrelated to the task (e.g., FitNet-R). This paper introduces three key innovations: 1) A frequency-domain decoupled teacher model that explicitly separates multi-scale spatiotemporal patterns. 2) A spectral-aligned distillation mechanism that mitigates cross-scale modeling biases in lightweight models. 3) A theoretical proof demonstrating the necessity of spectral knowledge transfer for learning long-range dependencies, providing an interpretable approach for lightweight spatiotemporal forecasting.

3. Method

3.1. Problem Formulation

Given a spatiotemporal sequence $X = \{X_t \in \mathbb{R}^{H \times W \times C}\}_{t=1}^T$, with $H \times W$ spatial grids and C channels, the forecasting task aims to predict future states $Y = \{X_{T+\tau}\}_{\tau=1}^{\Delta}$. Traditional methods minimize $\|F(X) - Y\|$, where F is a hybrid CNN-Transformer model. However, the quadratic complexity of Transformers $\mathcal{O}(N^2d)$ and deep CNNs limits deployment efficiency. Our goal is to distill F into a lightweight student \mathcal{G} with:

$$\min_{\theta_{\mathcal{G}}} \underbrace{|\mathcal{G}(X) - Y|}_{\text{Forecasting Loss}} + \lambda \underbrace{\mathcal{D}(\Psi(\mathcal{F}(X)), \Psi(\mathcal{G}(X)))}_{\text{Spectral Distillation Loss}}. \quad (1)$$

Here, Ψ extracts spectral features, and λ balances accuracy and efficiency.

3.2. Stage 1: Teacher Model Pretraining: Implicit Spectrum Decoupling

The teacher model \mathcal{F} uses the **Encoder-Latent Evolution-Decoder** architecture in Figure 1. It decouples frequency components in the latent space by cascading convolution and Transformer. We formalize it as follows:

$$Z = \mathcal{E}(X) \in \mathbb{R}^{H' \times W' \times D}. \quad (2)$$

The encoder \mathcal{E} maps the input sequence X to the latent space Z through multiple convolution layers. Then the latent evolution module processes Z with two parallel frequency-sensitive operations:

High-Frequency Extractor (CNN as High-Pass Filter)

$$Z^h = \text{ConvBlock}(Z) = \sigma(\text{Conv2D}(Z; \mathbf{W}_h) + b_h). \quad (3)$$

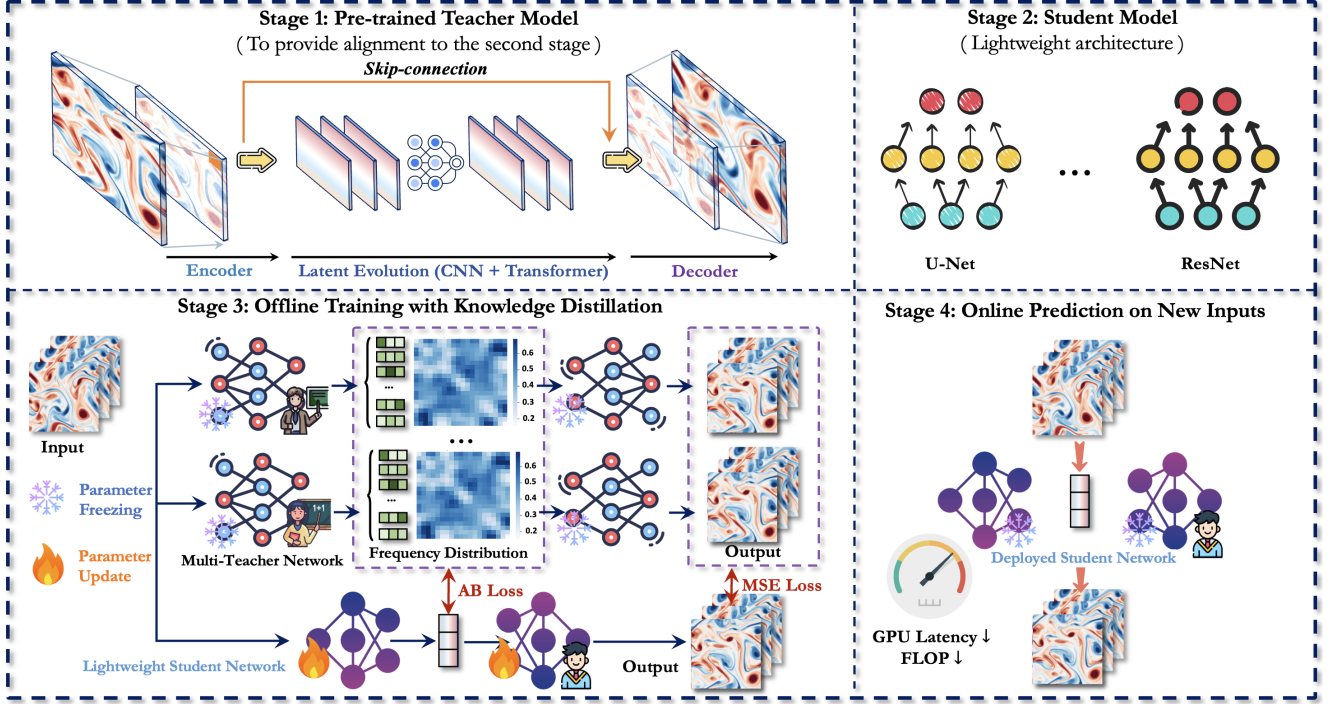


Figure 1. Architecture Overview of SDKD. **Stage 1:** Teacher model pretraining with frequency decoupling. **Stage 2:** Lightweight student architecture construction using parameter-efficient backbones like ResNet or U-Net. **Stage 3:** Offline Training with Knowledge Distillation. **Stage 4:** Online Prediction on New Inputs.

Here $\mathbf{W}_h \in \mathbb{R}^{K \times K \times D \times D}$ is the convolution kernel, and K is the local receptive field size. According to Park et al. [24], convolution layers perform implicit high-frequency filtering through local gradient operators $\nabla_{x,y}$:

$$\mathcal{F}_{\text{high}}(Z)(x, y) = \sum_{|\alpha| \leq k} a_\alpha \cdot \partial^\alpha Z(x, y). \quad (4)$$

The term α is the differentiation order, and a_α is a learnable parameter. This property helps CNN to effectively capture high-frequency details like abrupt traffic changes and turbulent vortices.

Low-Frequency Modeler (Transformer as Low-Pass Filter)

$$Z^l = \text{TransformerBlock}(Z) = \text{Softmax} \left(\frac{QK^T}{\sqrt{d}} \right) V. \quad (5)$$

Here $Q, K, V \in \mathbb{R}^{N \times d}$ are the query, key, and value matrices in self-attention, and $N = H' \times W'$ is the number of spatial positions. According to neural tangent kernel theory[13], self-attention acts like a low-pass filter:

$$\mathcal{F}_{\text{low}}(Z)(\omega) = \frac{1}{1 + \|\omega\|^2/\lambda} \cdot \hat{Z}(\omega). \quad (6)$$

The variable ω is the frequency component, and λ is the smoothing coefficient. This property helps the Transformer model low-frequency trends in meteorological evolution.

Latent State Fusion We fuse the high- and low-frequency components by a residual connection:

$$Z_{\text{evolved}} = \text{LayerNorm}(Z^h + Z^l). \quad (7)$$

Finally, the decoder \mathcal{D} reconstructs the prediction via deconvolution:

$$\hat{Y} = \mathcal{D}(Z_{\text{evolved}}). \quad (8)$$

This design ensures frequency decoupling in the latent space. According to Plancherel's theorem, the total error decomposes as:

$$\|\hat{Y} - Y\|^2 = \underbrace{\sum_{|\omega| > \omega_c} |\hat{Y}^h(\omega) - Y(\omega)|^2}_{\text{High-Frequency Error}} + \underbrace{\sum_{|\omega| \leq \omega_c} |\hat{Y}^l(\omega) - Y(\omega)|^2}_{\text{Low-Frequency Error}}. \quad (9)$$

Here ω_c is the cutoff frequency. By alternating the optimization of CNN and Transformer modules, the teacher

model minimizes both high- and low-frequency errors and provides ideal spectral priors for knowledge distillation.

Relation to Physical Laws: This architecture draws inspiration from the Navier-Stokes equations [17]. The high-frequency component corresponds to the viscous dissipation term $\nu \nabla^2 \mathbf{u}$, and the low-frequency component corresponds to the convection term $(\mathbf{u} \cdot \nabla) \mathbf{u}$. Experimental results (see Figure 2) show that the latent space aligns with the Kolmogorov energy spectrum $E(\omega) \propto \omega^{-5/3}$ in fluid dynamics, which confirms its physical interpretability.

3.3. Stage 2: Lightweight Student Architecture

To enable efficient deployment, we design a lightweight student model \mathcal{G} that can be flexibly instantiated as a simple CNN (e.g., ResNet), a U-Net, or even a multi-layer perceptron (MLP) with spatial reshaping. The key design goal is to avoid the heavy Transformer blocks and deep convolution stacks in the teacher model, drastically reducing parameter count and training memory while still maintaining adequate capacity for multi-scale spatiotemporal patterns.

Model Structure. Figure 1 (Stage 2) shows a compact variant that replaces the teacher’s complex latent evolution module with a shallower backbone, such as:

- **ResNet** [9]: A few residual blocks (3–4 layers each) for local feature extraction, enhanced by skip connections that help preserve gradient flow.
- **U-Net** [29]: An encoder-decoder with symmetric skip connections across scales to capture both coarse and fine spatial features.
- **MLP** [33]: Flatten (or reshape) the spatiotemporal grid and apply linear layers, suitable for extremely low-resource settings.

These backbones keep computational overhead to $\mathcal{O}(Nd)$ or $\mathcal{O}(Kd^2)$ rather than $\mathcal{O}(N^2d)$. Empirically, we set the hidden dimension d to be only 20%–30% that of the teacher, yielding a model up to $5\times$ smaller.

Compatibility with Teacher Outputs. The student architecture preserves the same input-output shapes as the teacher to ensure straightforward distillation. An initial convolution layer maps the multi-channel input sequence to the reduced hidden dimension d , feeding into the chosen lightweight backbone. Finally, a deconvolution (or reshaping) head reconstructs the forecast $\hat{Y}_s = \mathcal{G}(X)$. As detailed in Stage 3, we will align \hat{Y}_s with the teacher outputs at multiple spectral bands to guide the learning of crucial high-frequency details and low-frequency trends.

3.4. Stage 3: Offline Training with Knowledge Distillation

After pretraining a frequency-decoupled teacher and designing a lightweight student, we perform offline training under a knowledge distillation framework. Suppose we have one

or more teacher networks, each of which has been trained with the convolution-Transformer “high-frequency vs. low-frequency” decoupling mechanism.

3.4.1. Frequency-Aligned Distillation

For a single teacher, our focus is on transferring the teacher’s multi-scale spectral embeddings into the student. Specifically, produces latent representations containing high-frequency and low-frequency components. We extract these frequency-specific features and construct the *spectral transfer loss*:

$$\mathcal{L}_{\text{KD}} = \|\Psi_h(\mathcal{G}(X)) - \Psi_h(\mathcal{F}(X))\|_2^2 + \alpha \|\Psi_l(\mathcal{G}(X)) - \Psi_l(\mathcal{F}(X))\|_2^2, \quad (10)$$

here, α balances the focus on aligning high and low frequencies. Meanwhile, we also minimize the student’s loss on the forecasting target. Thus, the overall optimization objective is:

$$\min_{\theta_{\mathcal{G}}} \left(\|\mathcal{G}(X) - Y\|_2^2 + \lambda \mathcal{L}_{\text{KD}} \right), \quad (11)$$

here, λ is a hyperparameter that balances the forecasting error and the distillation loss.

3.4.2. Multi-Teacher Distillation

We can have multiple teacher models $\{\mathcal{F}_1, \dots, \mathcal{F}_M\}$, each excelling in different spatial/frequency domains or physical environments. Simply averaging all teacher outputs or features may lead to information loss [44] when conflicts or differences exist among teachers. To better leverage their complementarity, we adopt the *Agree to Disagree (A2D)* method proposed by Du et al. [7], treating multi-teacher distillation as a small-scale **multi-objective optimization** problem. In each iteration, we solve a subproblem in the gradient space to adaptively weight the teacher gradients.

(1) Define the distillation loss for each teacher. For the m th teacher \mathcal{F}_m , define its frequency alignment distillation loss as:

$$\ell_m(\theta_{\mathcal{G}}) = \|\mathcal{G}(X) - Y\|^2 + \lambda \|\Psi(\mathcal{G}(X)) - \Psi(\mathcal{F}_m(X))\|^2, \quad (12)$$

Here, $\Psi(\cdot)$ extracts features and aligns them in the frequency domain. Each teacher provides a loss signal ℓ_m .

(2) Perform multi-objective optimization in the gradient space. A2D solves the teacher gradient weighting coefficients $\{\alpha_m\}$ on the “capped simplex” [7] during each mini-batch update using the following equation:

$$\begin{aligned} \min_{\{\alpha_m\}} \quad & \frac{1}{2} \left\| \sum_{m=1}^M \alpha_m \nabla_{\theta} \ell_m \right\|^2 \\ \text{s.t.} \quad & \sum_{m=1}^M \alpha_m = 1, \quad 0 \leq \alpha_m \leq C. \end{aligned} \quad (13)$$

Here, $C \in (0, 1]$ is a hyperparameter that controls the tolerance for divergence among teachers.

(3) Update the student network parameters. Let α_m^* be the optimal solution obtained from the above equation. The student updates its parameters using the following gradient descent direction:

$$d = - \sum_{m=1}^M \alpha_m^* \nabla_{\theta} \ell_m. \quad (14)$$

Let the learning rate be η , then the student updates its parameters as:

$$\theta_G \leftarrow \theta_G - \eta d. \quad (15)$$

In this process, each teacher’s influence on the student is dynamically determined by α_m^* . If a teacher’s gradient direction conflicts significantly with others, its weight decreases accordingly. This avoids "blind averaging" while effectively preserving useful information from most teachers. By introducing A2D, frequency alignment distillation in multi-teacher scenarios no longer relies on simple averaging of all teacher features or outputs. Instead, it adaptively assigns weights at the gradient level. This approach fully leverages each teacher’s strengths in modeling different frequency bands (high/low) or scenarios, improving the student model’s overall forecasting ability.

3.5. Stage 4: Prediction with Lightweight Student

After training, the student model \mathcal{G} is deployed for online inference. Given a new input sequence X_{new} , the prediction is generated in a single forward pass:

$$\hat{Y}_{\text{new}} = \mathcal{G}(X_{\text{new}}) \in \mathbb{R}^{H \times W \times C \times \Delta}. \quad (16)$$

The lightweight architecture removes the teacher’s quadratic-complexity Transformer blocks and deep convolution stacks. For example, on the NS equation dataset, inference speed increases by $2.28 \times$ compared to the teacher. Importantly, frequency-aligned knowledge from distillation enables \mathcal{G} to keep multi-scale modeling capability: local convolutions approximate high-frequency patterns learned from the teacher’s CNN module, and residual connections propagate global trends similar to attention mechanisms. This approach ensures accurate predictions under both steady-state and transient disturbances without explicit frequency transforms, achieving an optimal balance between efficiency and spectral fidelity (see Figure 1).

4. Experiment

4.1. Experimental Settings

Benchmarks. As shown in Table 2, we use a wide range of scenarios to evaluate our model which includes four datasets. Here are the descriptions of these datasets.

Table 2. Detailed information for benchmarks. N_{tr} , N_{ev} and N_{te} represent the number of instances in the training, evaluation, and test sets, while I_l and O_l denote the lengths of the input and prediction sequences, respectively. N_v denotes the number of variables.

Dataset	N_{tr}	N_{ev}	N_{te}	N_v	Resolution	I_l	O_l	Interval
RBC	35,718	4,465	4,465	1	(32, 480)	13	12	5 mins
TaxiBJ+	1,660	208	208	2	(128, 128)	5	15	1 day
WeatherBench	4,158	445	500	3	(32, 64)	6	36	1 hour
NSE	1,000	100	100	1	(64, 64)	10	10	1 step

Table 3. Distillation performance on Weatherbench and TaxiBJ+ with MAE, PSNR, SSIM, MSE, MAE, and SSIM.

Method	Weatherbench			TaxiBJ+		
	MAE	PSNR	SSIM	MSE	MAE	SSIM
T ₁ : ST-AlterNet	0.7287	33.3219	0.9493	0.0683	0.1172	0.9701
T ₂ : SimVP	0.7475	32.1124	0.9331	0.0697	0.1233	0.9653
S: U-Net	0.9822	29.3741	0.8635	0.0831	0.1354	0.9532
+AVER-MKD (<i>w AB loss</i>)	0.8541	31.4527	0.8812	0.0728	0.1241	0.9624
+AEKD (<i>w AB loss</i>)	0.8925	30.7843	0.8724	0.0753	0.1279	0.9587
+AEKD (<i>w MSE loss</i>)	0.8457	31.6921	0.8849	0.0715	0.1228	0.9639
S: ResNet	0.9645	30.0192	0.8662	0.0876	0.1421	0.9483
+AEKD (<i>w AB loss</i>)	0.9218	30.5124	0.8753	0.0802	0.1337	0.9549
+AEKD (<i>w MSE loss</i>)	0.9102	30.8237	0.8801	0.0784	0.1305	0.9572
S: MLP-Mixer	1.1826	24.9732	0.7821	0.0953	0.1527	0.9375
+AEKD (<i>w AB loss</i>)	1.1534	25.2175	0.7879	0.0918	0.1473	0.9402
+AEKD (<i>w MSE loss</i>)	1.1428	25.3216	0.7893	0.0901	0.1452	0.9427

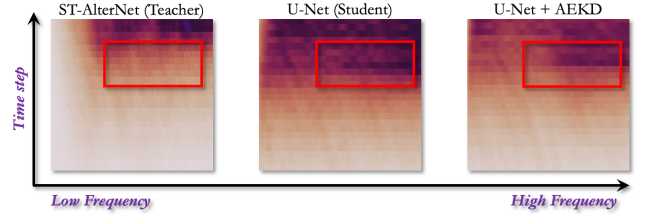


Figure 2. Spectral characteristics analysis in the Weatherbench dataset.

- Rayleigh-Bénard Convection(RBC)** [37] is calculated by the Lattice Boltzmann Method to solve the 2-d fluid thermodynamics equations for two-dimensional turbulent flow.
- TaxiBJ+** [36] is a spatiotemporal traffic flow dataset derived from GPS trajectories of taxis in Beijing. It divides the city into grid regions and records inflow and outflow every 30 minutes, forming a temporal-spatial data stream. Covering a long time span (e.g., 2013–2016), it includes various travel scenarios such as weekdays, weekends, and holidays, making it a widely used benchmark for evaluating spatiotemporal forecasting models.
- WeatherBench** [20] selects 2,048 grid points ($H \times W = 32 \times 64$) on the Earth’s sphere and provides hourly meteorological data. The experiment uses four variables: temperature (K), cloud cover ($\% \times 10^1 - 1$), humidity ($\% \times 10$), and surface wind speed components (ms^{-1}).

The data spans from January 1, 2010, to December 31, 2018. Both input and forecast time lengths are set to 12 hours.

- Navier-Stokes Equation (NSE)** [17] describes the dynamics and mass transport of the general fluid. We select the two-dimensional equations for an incompressible viscous fluid with a viscosity coefficient of 10^{-5} to test our model for learning complicated fluid dynamics with high Reynolds numbers.

Table 4. Performance Comparison on NS Dataset with U-Net Student Model. The table presents MSE, MAE, and SSIM scores for various methods, highlighting the best-performing ones with a checkmark (green) and the worst with a cross (red). Bold indicates best performance.

METHOD	MSE	MAE	SSIM	OVERALL
BASELINE (S)	0.141	0.239	0.658	–
AVER-MKD	0.136	0.233	0.670	✓
AEKD	0.135	0.235	0.663	✓
CAMKD	0.136	0.234	0.667	✓

Table 5. Performance Comparison on RBC Dataset with U-Net Student Model. This table compares MSE, MAE, SSIM, and overall performance, with the best results marked by a green checkmark and the worst by a red cross. Bold indicates best performance.

METHOD	MSE	MAE	SSIM	OVERALL
BASELINE (S)	0.0267	0.114	0.723	–
AVER-MKD	0.0264	0.114	0.726	✓
AEKD (w ABLOSS)	0.0281	0.118	0.714	✗
CAMKD	0.0261	0.112	0.728	✓
SINGLE TEACHER (VAN)	0.0265	0.114	0.726	✓

Table 6. Performance Comparison on RBC Dataset with ResNet Student Model. MSE, MAE, and SSIM are reported, with the best methods marked with a green checkmark and the worst with a red cross. Bold indicates best performance.

METHOD	MSE	MAE	SSIM	OVERALL
BASELINE (S)	0.0356	0.132	0.686	–
AEKD (w ABLOSS)	0.0395	0.139	0.675	✗
CAMKD	0.0331	0.125	0.706	✓

Teacher Models: We use two advanced neural network architectures as teacher networks. The detailed descriptions are as follows.

- ST-AlterNet (T₁):** Our proposed teacher algorithm combines Transformer and CNN in a serial architecture. The

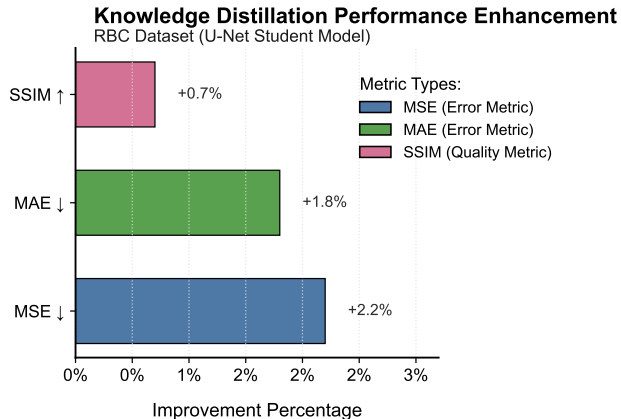


Figure 3. Performance improvement percentage on the RBC Dataset (U-Net Student Model).

model first extracts local spatial features through convolutional layers, then captures global temporal dependencies via multi-head self-attention mechanisms. This hybrid design enables joint modeling of short-range and long-range spatiotemporal patterns.

- SimVP (T₂):** As baseline teacher model, we adopt the standard SimVP architecture [8] which implements pure convolutional operations for video prediction. Its deep hierarchical structure with temporal skip connections serves as a strong spatial-temporal feature extractor.

Student Models: We select three lightweight neural network architectures as student networks. The descriptions are as follows, with the core code provided in the appendix.

- U-Net:** Selected for its encoder-decoder structure with skip connections, particularly effective in preserving fine-grained spatial details through symmetric contracting and expanding paths.
- ResNet:** Utilizes residual blocks with identity mappings to enable stable training of deep networks. The bottleneck design balances computational efficiency and feature representation capacity.
- MLP-Mixer:** Adopts the isotropic architecture that processes spatial and temporal tokens through parallel MLP layers, providing a parameter-efficient baseline without inductive bias.

Distillation Strategy. We implement two knowledge transfer frameworks:

- AVER-MKD [11]:** A baseline method for multi-teacher knowledge distillation that guides the student model by averaging the outputs of all teachers.
- AEKD [7]:** The baseline adaptive ensemble knowledge distillation method, implemented with two loss variants:
 - AB Loss [10]:** Adversarial boundary-aware loss that emphasizes transitional regions.
 - MSE Loss:** Standard mean squared error based feature matching

Implementation. Based on the above experimental setup, all our experiments are conducted on two NVIDIA GeForce RTX 4090 GPUs. For the knowledge distillation part, we add AB Loss or MSE Loss in addition to the task-supervised MSE loss, forming a composite loss to better fit the teacher model’s feature distribution. All models use the Adam optimizer with a fixed learning rate of 1×10^{-4} , trained for 300 epochs, and early stopping is applied based on monitoring the loss on the validation set. We use PyTorch’s default parameter initialization and set the random seed to 42 to ensure reproducibility. The model weights with the best performance on the validation set are retained for the testing phase.

4.2. Main Results

The Table 3 shows the distillation performance on the Weatherbench and TaxiBJ+ datasets. We compare different teacher models (T_1 : ST-AlterNet and T_2 : SimVP) with student models. ST-AlterNet outperforms SimVP, especially on Weatherbench, with better MAE, PSNR, and SSIM values. Next, we compare student models trained with different distillation strategies like AVER-MKD and AEKD. U-Net, ResNet, and MLP-Mixer all show better performance with AEKD (especially with AB Loss or MSE Loss). For example, U-Net with AEKD (w AB Loss) achieves MAE of 0.8541, PSNR of 31.4527, and SSIM of 0.8812. ResNet and MLP-Mixer also improve in MAE and SSIM after AEKD distillation. In summary, AEKD helps student models perform better by transferring spectral features from the teacher model. It maintains a good balance between efficiency and accuracy.

4.3. Spectral characteristics analysis

As shown in the Figure 2, the teacher model ST-AlterNet has lower prediction errors in both low and high-frequency regions, demonstrating balanced modeling of the multi-scale evolution of meteorological systems. In contrast, the U-Net student model without distillation exhibits higher errors, especially in the high-frequency region. This suggests that the original U-Net struggles to effectively capture high-frequency information, highlighting the limitations of its simple convolutional structure in modeling cross-scale interactions—over-smoothing leads to a shift in low-frequency trends, while high-frequency transient features (e.g., thunderstorm boundaries) are distorted. After spectral decoupling distillation (SDKD), the student model’s low and high-frequency errors significantly decrease, approaching the teacher model’s performance. This improvement is attributed to the two-stage distillation mechanism: (1) *Low-frequency alignment*: By transferring the attention weight matrix of the teacher’s Transformer module, the student model learns the global meteorological field evolution rules through its residual connections. (2) *High-frequency enhancement*: Using the teacher’s latent space multi-scale

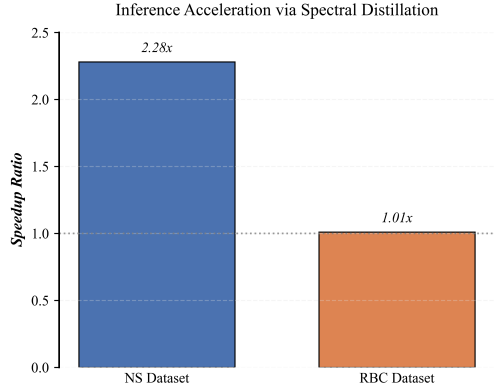


Figure 4. Inference speedup comparison between teacher and distilled student models.

features as supervision, the student model’s shallow convolution kernels focus on local perturbation patterns, thereby reducing high-frequency errors.

4.4. Distillation Method Analysis

As shown in Tables 4, 5, 6, we compare the performance of different distillation methods on the NS and RBC datasets. The baseline method (S) performs poorly, with MSE and MAE of 0.141 and 0.239 (NS dataset), and 0.0267 and 0.114 (RBC dataset), respectively. AVER-MKD and AEKD improve performance on both datasets, with AVER-MKD reducing MSE on the RBC dataset to 0.0264, MAE to 0.114, and increasing SSIM to 0.726. However, CAMKD performs the best, with an MSE of 0.0261, MAE of 0.112, and SSIM of 0.728 on the RBC dataset, showing the best cross-scale modeling ability. CAMKD reduces high-frequency errors and improves low-frequency trend modeling accuracy through multi-teacher distillation and spectral alignment mechanisms, delivering the best predictive performance.

4.5. Efficiency Analysis

In this section, as shown in Figure 4, we compare the inference speeds of the teacher model and the distilled student model. On the NS dataset, the teacher model (SimVP) takes 0.0115 seconds, while the distilled U-Net student model takes 0.0050 seconds, nearly halving the inference time. On the RBC dataset, the teacher model (SimVP) takes 0.0192 seconds, while the distilled U-Net student model takes 0.0189 seconds, offering a smaller yet still notable speedup. The slower speed on the RBC dataset is mainly due to its higher resolution. This indicates that while the gap on the RBC dataset is smaller, the distillation method provides a more significant acceleration on the NS dataset.

5. Conclusion

In summary, our proposed spectral decoupling knowledge distillation framework achieves excellent prediction performance on multiple datasets. It significantly improves the lightweight student model’s ability to capture multi-scale features, including high-frequency details and low-frequency trends. It explicitly aligns the teacher model’s spectral information and distills it to the student. This approach resolves the original model’s limitations in cross-scale feature learning. It achieves or nearly matches the teacher model’s accuracy while reducing inference time. Our findings reveal that this spectral decoupling distillation paradigm has strong applicability and expansion potential in spatiotemporal forecasting, offering new insights and technical support for future research on multi-scale spatiotemporal modeling and deployment.

6. Acknowledgements

This work is partially supported by the National Natural Science Foundation of China under Grant Number 62476264 and 62406312, the Postdoctoral Fellowship Program and China Postdoctoral Science Foundation under Grant Number BX20240385 (China National Postdoctoral Program for Innovative Talents), and the Science Foundation of the Chinese Academy of Sciences.

References

- [1] Antonio A Abello, Roberto Hirata, and Zhangyang Wang. Dissecting the high-frequency bias in convolutional neural networks. In *Proceedings of the IEEE/CVF Conference on Computer Vision and Pattern Recognition*, pages 863–871, 2021. 2
- [2] Kaifeng Bi, Lingxi Xie, Hengheng Zhang, Xin Chen, Xiaotao Gu, and Qi Tian. Accurate medium-range global weather forecasting with 3d neural networks. *Nature*, 619(7970):533–538, 2023. 1
- [3] Shuhao Cao. Choose a transformer: Fourier or galerkin. *Advances in neural information processing systems*, 34:24924–24940, 2021. 3
- [4] Yuan Cao, Zhiying Fang, Yue Wu, Ding-Xuan Zhou, and Quanquan Gu. Towards understanding the spectral bias of deep learning. *arXiv preprint arXiv:1912.01198*, 2019. 2
- [5] Yuning Cui, Yi Tao, Zhenshan Bing, Wenqi Ren, Xinwei Gao, Xiaochun Cao, Kai Huang, and Alois Knoll. Selective frequency network for image restoration. In *The Eleventh International Conference on Learning Representations*, 2023. 3
- [6] Matthew F Dixon, Nicholas G Polson, and Vadim O Sokolov. Deep learning for spatio-temporal modeling: dynamic traffic flows and high frequency trading. *Applied Stochastic Models in Business and Industry*, 35(3):788–807, 2019. 1
- [7] Shangchen Du, Shan You, Xiaojie Li, Jianlong Wu, Fei Wang, Chen Qian, and Changshui Zhang. Agree to disagree: Adaptive ensemble knowledge distillation in gradient space. *advances in neural information processing systems*, 33:12345–12355, 2020. 5, 7
- [8] Zhangyang Gao, Cheng Tan, Lirong Wu, and Stan Z Li. Simvp: Simpler yet better video prediction. In *Proceedings of the IEEE/CVF Conference on Computer Vision and Pattern Recognition*, pages 3170–3180, 2022. 7
- [9] Kaiming He, Xiangyu Zhang, Shaoqing Ren, and Jian Sun. Deep residual learning for image recognition. In *Proceedings of the IEEE conference on computer vision and pattern recognition*, pages 770–778, 2016. 5
- [10] Byeongho Heo, Minsik Lee, Sangdoon Yun, and Jin Young Choi. Knowledge transfer via distillation of activation boundaries formed by hidden neurons. In *Proceedings of the AAAI conference on artificial intelligence*, pages 3779–3787, 2019. 7
- [11] Geoffrey Hinton. Distilling the knowledge in a neural network. *arXiv preprint arXiv:1503.02531*, 2015. 3, 7
- [12] Mohammad Izadi, Mehran Safayani, and Abdolreza Mirzaei. Knowledge distillation on spatial-temporal graph convolutional network for traffic prediction. *International Journal of Computers and Applications*, pages 1–12, 2024. 3
- [13] Arthur Jacot, Franck Gabriel, and Clément Hongler. Neural tangent kernel: Convergence and generalization in neural networks. *Advances in neural information processing systems*, 31, 2018. 3, 4
- [14] Mingi Ji, Byeongho Heo, and Sungrae Park. Show, attend and distill: Knowledge distillation via attention-based feature matching. In *Proceedings of the AAAI Conference on Artificial Intelligence*, pages 7945–7952, 2021. 3
- [15] Weiwei Jiang and Jiayun Luo. Graph neural network for traffic forecasting: A survey. *Expert Systems with Applications*, 207:117921, 2022. 1
- [16] Amin Karimi Monsefi, Mengxi Zhou, Nastaran Karimi Monsefi, Ser-Nam Lim, Wei-Lun Chao, and Rajiv Ramnath. Frequency-guided masking for enhanced vision self-supervised learning. *arXiv e-prints*, pages arXiv–2409, 2024. 3
- [17] Zongyi Li, Nikola Kovachki, Kamyar Aizzadenesheli, Burigede Liu, Kaushik Bhattacharya, Andrew Stuart, and Anima Anandkumar. Fourier neural operator for parametric partial differential equations. *arXiv preprint arXiv:2010.08895*, 2020. 2, 3, 5, 7
- [18] Zheng Li, Xiang Li, Lingfeng Yang, Borui Zhao, Renjie Song, Lei Luo, Jun Li, and Jian Yang. Curriculum temperature for knowledge distillation. In *Proceedings of the AAAI Conference on Artificial Intelligence*, pages 1504–1512, 2023. 3
- [19] Zheng Li, Xiang Li, Xinyi Fu, Xin Zhang, Weiqiang Wang, Shuo Chen, and Jian Yang. Promptkd: Unsupervised prompt distillation for vision-language models. In *Proceedings of the IEEE/CVF Conference on Computer Vision and Pattern Recognition*, pages 26617–26626, 2024. 3
- [20] Haitao Lin, Zhangyang Gao, Yongjie Xu, Lirong Wu, Ling Li, and Stan Z Li. Conditional local convolution for spatiotemporal meteorological forecasting. In *Proceedings of the AAAI Conference on Artificial Intelligence*, pages 7470–7478, 2022. 6

- [21] Zhiyu Lin, Yifei Gao, and Jitao Sang. Investigating and explaining the frequency bias in image classification. *arXiv preprint arXiv:2205.03154*, 2022. 2
- [22] Nikola Milojevic-Dupont and Felix Creutzig. Machine learning for geographically differentiated climate change mitigation in urban areas. *Sustainable Cities and Society*, 64:102526, 2021. 1
- [23] Zheyi Pan, Yuxuan Liang, Weifeng Wang, Yong Yu, Yu Zheng, and Junbo Zhang. Urban traffic prediction from spatio-temporal data using deep meta learning. In *Proceedings of the 25th ACM SIGKDD international conference on knowledge discovery & data mining*, pages 1720–1730, 2019. 1
- [24] Namuk Park and Songkuk Kim. How do vision transformers work? *arXiv preprint arXiv:2202.06709*, 2022. 2, 4
- [25] Cuong Pham, Van-Anh Nguyen, Trung Le, Dinh Phung, Gustavo Carneiro, and Thanh-Toan Do. Frequency attention for knowledge distillation. In *Proceedings of the IEEE/CVF Winter Conference on Applications of Computer Vision*, pages 2277–2286, 2024. 3
- [26] Maithra Raghu, Thomas Unterthiner, Simon Kornblith, Chiyuan Zhang, and Alexey Dosovitskiy. Do vision transformers see like convolutional neural networks? *Advances in neural information processing systems*, 34:12116–12128, 2021. 2
- [27] Nasim Rahaman, Aristide Baratin, Devansh Arpit, Felix Draxler, Min Lin, Fred Hamprecht, Yoshua Bengio, and Aaron Courville. On the spectral bias of neural networks. In *International conference on machine learning*, pages 5301–5310. PMLR, 2019. 2
- [28] Adriana Romero, Nicolas Ballas, Samira Ebrahimi Kahou, Antoine Chassang, Carlo Gatta, and Yoshua Bengio. Fitnets: Hints for thin deep nets. *arXiv preprint arXiv:1412.6550*, 2014. 2, 3
- [29] Olaf Ronneberger, Philipp Fischer, and Thomas Brox. U-net: Convolutional networks for biomedical image segmentation. In *Medical image computing and computer-assisted intervention—MICCAI 2015: 18th international conference, Munich, Germany, October 5–9, 2015, proceedings, part III 18*, pages 234–241. Springer, 2015. 5
- [30] Arjun Sarkar. Understanding depthwise separable convolutions and the efficiency of mobilenets. *Towards Data Science*, 2021. 2
- [31] Xingjian Shi, Zhoung Chen, Hao Wang, Dit-Yan Yeung, Wai-Kin Wong, and Wang-chun Woo. Convolutional lstm network: A machine learning approach for precipitation now-casting. *Advances in neural information processing systems*, 28, 2015. 1, 3
- [32] AJ Simmons, P Poli, DP Dee, P Berrisford, H Hersbach, S Kobayashi, and C Peubey. Estimating low-frequency variability and trends in atmospheric temperature using era-interim. *Quarterly Journal of the Royal Meteorological Society*, 140(679):329–353, 2014. 1
- [33] Ilya O Tolstikhin, Neil Houlsby, Alexander Kolesnikov, Lucas Beyer, Xiaohua Zhai, Thomas Unterthiner, Jessica Yung, Andreas Steiner, Daniel Keysers, Jakob Uszkoreit, et al. Mlp-mixer: An all-mlp architecture for vision. *Advances in neural information processing systems*, 34:24261–24272, 2021. 5
- [34] Haohan Wang, Xindi Wu, Zeyi Huang, and Eric P Xing. High-frequency component helps explain the generalization of convolutional neural networks. In *Proceedings of the IEEE/CVF conference on computer vision and pattern recognition*, pages 8684–8694, 2020. 2
- [35] Yunbo Wang, Mingsheng Long, Jianmin Wang, Zhifeng Gao, and Philip S Yu. Predrnn: Recurrent neural networks for predictive learning using spatiotemporal lstms. *Advances in neural information processing systems*, 30, 2017. 1, 3
- [36] Hao Wu, Yuxuan Liang, Wei Xiong, Zhengyang Zhou, Wei Huang, Shilong Wang, and Kun Wang. Earthfarsser: Versatile spatio-temporal dynamical systems modeling in one model. In *Proceedings of the AAAI Conference on Artificial Intelligence*, pages 15906–15914, 2024. 1, 3, 6
- [37] Hao Wu, Kangyu Weng, Shuyi Zhou, Xiaomeng Huang, and Wei Xiong. Neural manifold operators for learning the evolution of physical dynamics. In *Proceedings of the 30th ACM SIGKDD Conference on Knowledge Discovery and Data Mining*, pages 3356–3366, 2024. 6
- [38] Hao Wu, Fan Xu, Chong Chen, Xian-Sheng Hua, Xiao Luo, and Haixin Wang. Pastnet: Introducing physical inductive biases for spatio-temporal video prediction. In *Proceedings of the 32nd ACM International Conference on Multimedia*, pages 2917–2926, 2024. 1
- [39] Chuanguang Yang, Zhulin An, Linhang Cai, and Yongjun Xu. Hierarchical self-supervised augmented knowledge distillation. In *Proceedings of the Thirtieth International Joint Conference on Artificial Intelligence*, pages 1217–1223, 2021. 1
- [40] Chuanguang Yang, Zhulin An, Linhang Cai, and Yongjun Xu. Mutual contrastive learning for visual representation learning. In *Proceedings of the AAAI Conference on Artificial Intelligence*, pages 3045–3053, 2022. 1
- [41] Chuanguang Yang, Helong Zhou, Zhulin An, Xue Jiang, Yongjun Xu, and Qian Zhang. Cross-image relational knowledge distillation for semantic segmentation. In *Proceedings of the IEEE/CVF conference on computer vision and pattern recognition*, pages 12319–12328, 2022. 3
- [42] Chuanguang Yang, Zhulin An, Helong Zhou, Fuzhen Zhuang, Yongjun Xu, and Qian Zhang. Online knowledge distillation via mutual contrastive learning for visual recognition. *IEEE Transactions on Pattern Analysis and Machine Intelligence*, 45(8):10212–10227, 2023. 1
- [43] Chuanguang Yang, Zhulin An, Libo Huang, Junyu Bi, Xinqiang Yu, Han Yang, Boyu Diao, and Yongjun Xu. Clip-kd: An empirical study of clip model distillation. In *Proceedings of the IEEE/CVF Conference on Computer Vision and Pattern Recognition*, pages 15952–15962, 2024. 3
- [44] Chuanguang Yang, Xinqiang Yu, Han Yang, Zhulin An, Chengqing Yu, Libo Huang, and Yongjun Xu. Multi-teacher knowledge distillation with reinforcement learning for visual recognition. In *Proceedings of the AAAI Conference on Artificial Intelligence*, pages 9148–9156, 2025. 5
- [45] Chengting Yu, Fengzhao Zhang, Ruizhe Chen, Aili Wang, Zuozhu Liu, Shurun Tan, and Er-Ping Li. Decoupling dark knowledge via block-wise logit distillation for feature-level alignment. *IEEE Transactions on Artificial Intelligence*, 2024. 2

- [46] Chengqing Yu, Fei Wang, Zezhi Shao, Tangwen Qian, Zhao Zhang, Wei Wei, Zhulin An, Qi Wang, and Yongjun Xu. Ginar+: A robust end-to-end framework for multivariate time series forecasting with missing values. *IEEE Transactions on Knowledge and Data Engineering*, 2025. [1](#)
- [47] Chengqing Yu, Fei Wang, Chuanguang Yang, Zezhi Shao, Tao Sun, Tangwen Qian, Wei Wei, Zhulin An, and Yongjun Xu. Merlin: Multi-view representation learning for robust multivariate time series forecasting with unfixed missing rates. *arXiv preprint arXiv:2506.12459*, 2025. [1](#)
- [48] Yuchen Zhang, Mingsheng Long, Kaiyuan Chen, Lanxiang Xing, Ronghua Jin, Michael I Jordan, and Jianmin Wang. Skilful nowcasting of extreme precipitation with nowcastnet. *Nature*, 619(7970):526–532, 2023. [1](#)
- [49] Yuan Zhang, Tao Huang, Jiaming Liu, Tao Jiang, Kuan Cheng, and Shanghang Zhang. Freekd: Knowledge distillation via semantic frequency prompt. In *Proceedings of the IEEE/CVF Conference on Computer Vision and Pattern Recognition*, pages 15931–15940, 2024. [2](#)